



Multimodal analysis of formalin-fixed and paraffin-embedded tissue by MALDI imaging and fluorescence in situ hybridization for combined genetic and metabolic analysis

Katharina Huber¹ · Thomas Kunzke¹ · Achim Buck¹ · Rupert Langer² · Birgit Luber³ · Annette Feuchtinger¹ · Axel Walch¹

Received: 18 January 2019 / Revised: 30 April 2019 / Accepted: 30 April 2019 / Published online: 31 May 2019

© United States & Canadian Academy of Pathology 2019

Abstract

Multimodal tissue analyses that combine two or more detection technologies provide synergistic value compared to single methods and are employed increasingly in the field of tissue-based diagnostics and research. Here, we report a technical pipeline that describes a combined approach of HER2/CEP17 fluorescence in situ hybridization (FISH) analysis with MALDI imaging on the very same section of formalin-fixed and paraffin-embedded (FFPE) tissue. FFPE biopsies and a tissue microarray of human gastroesophageal adenocarcinoma were analyzed by MALDI imaging. Subsequently, the very same section was hybridized by HER2/CEP17 FISH. We found that tissue morphology of both, the biopsies and the tissue microarray, was unaffected by MALDI imaging and the HER2 and CEP17 FISH signals were analyzable. In comparison with FISH analysis of samples without MALDI imaging, we observed no difference in terms of fluorescence signal intensity and gene copy number. Our combined approach revealed adenosine monophosphate, measured by MALDI imaging, as a prognostic marker. HER2 amplification, which was detected by FISH, is a stratifier between good and poor patient prognosis. By integrating both stratification parameters on the basis of our combined approach, we were able to strikingly improve the prognostic effect. Combining molecules detected by MALDI imaging with the gene copy number detected by HER2/CEP17 FISH, we found a synergistic effect, which enhances patient prognosis. This study shows that our combined approach allows the detection of genetic and metabolic properties from one very same FFPE tissue section, which are specific for HER2 and hence suitable for prognosis. Furthermore, this synergism might be useful for response prediction in tumors.

Introduction

The present work describes a combined method for the multimodal analysis of one very same tissue section. The

addition of two or more technologies enables a new way of analysis, which adds further information for diagnosis, treatment, and monitoring [1, 2]. It has been demonstrated that the addition of a further modality can drastically enhance information gain in tissue-based analysis [3]. In clinical research, there are numerous developments especially in the field of multimodal molecular imaging, which promise to improve treatment strategy, targeted therapy, and personalized medicine [1].

In this study, MALDI imaging is added as a further modality to the genetic FISH analysis.

MALDI imaging is an emerging tool for the investigation of proteins, peptides, lipids, metabolites, small molecules, and many other classes in a spatially resolved manner [4–6]. Meanwhile, MALDI imaging is a technology suitable for diagnostics and for predictive approaches, which is unique in providing molecular information with spatial resolution [7]. Previously matrix-assisted laser desorption ionization (MALDI) imaging was established

These authors contributed equally: Katharina Huber, Thomas Kunzke

Supplementary information The online version of this article (<https://doi.org/10.1038/s41374-019-0268-z>) contains supplementary material, which is available to authorized users.

✉ Axel Walch
axel.walch@helmholtz-muenchen.de

¹ Research Unit Analytical Pathology, Helmholtz Zentrum München, German Research Center for Environmental Health, Neuherberg, Germany

² Institute of Pathology, University of Bern, Bern, Switzerland

³ Institute of Pathology, Technische Universität München, Munich, Germany

for the metabolic analysis of formalin-fixed and paraffin-embedded (FFPE) tissues [8]. This achievement enables analysis of the metabolic content of large tissue banks and clinical samples, which are usually preserved and stored as paraffin blocks.

The employment of a further measurement modality without further need of tissue, but in just using one very same tissue section for several analyses, seems meaningful, especially in the context of limited human diagnostic material. Although method combination with MALDI imaging seems promising, there are only few studies, which have already used MALDI imaging for multimodal approaches. An example is the proteomic analysis by MALDI imaging combined with receptor staining by immunohistochemistry using one very same tissue section for both modalities [7].

In cancer treatment, the examination of drug targets is an important tool for estimation of drug efficiency and therapy response [9]. The human epithelial growth factor receptor 2 (HER2) is a receptor, which is overexpressed in several cancer types such as breast cancer and gastroesophageal adenocarcinoma [9, 10]. Thus, HER2 serves as a drug target and the binding antibody, known as Trastuzumab, is in wide use as a cancer therapeutic [10]. As targeting HER2 is only successful when overexpressed, HER2 testing by immunohistochemistry (IHC) and fluorescence in situ hybridization (FISH) is a routine method in diagnosing the respective cancer diseases [11].

State of the art in HER2 diagnosis is immunohistochemical staining and in situ hybridization [12]. The immunohistochemical staining, directly labeling HER2, is scored as 0, 1+, 2+, or 3+. Score 0 and 1+ are defined as HER2 negative, which means anti-HER2 treatment is not considered at all, and 3+ is HER2 positive, an outcome, which recommends anti-HER2 treatment. The score 2+ represents an intermediate state, which requires further testing. In this case in situ hybridization is performed as fluorescence or chromogenic in situ hybridization. Hereby the signals of labeled gene copies are counted in at least 20 tumor cell nuclei and a ratio of gene copy number and chromosome number is calculated and defined as amplified when the ratio is ≥ 2 . Samples with a ratio of 2 or more are then also defined as HER2 positive and this leads to an HER2 directed treatment [11–13].

In HER2 testing, FISH is an FDA approved method for the enumeration of the absolute HER2 gene copy number in breast cancer and gastroesophageal adenocarcinoma [11, 14–16]. Nonetheless, there is still potential for improving diagnostics and response prediction for HER2 directed treatments. There is a subgroup of HER2-positive cancer patients, which do not respond to anti-HER2 treatment and hence the patients do not profit from yet very cost

intensive medication but undergo the risk of side effects [17–21].

Thus, the integration of additional metabolic markers may lead to a better prognosis. Tumor growth and progression is an energy demanding process, consuming high amounts of adenosine triphosphate (ATP) [22]. If ATP supply is not sufficient, adenosine monophosphate levels rise and activate adenosine monophosphate-activated kinase (AMPK), which induces catabolic pathways to support ATP production [22]. High AMP levels are described to activate AMPK, which further activates pathways that are involved in tumor growth, autophagy, and metabolism [23–25]. Hence, the AMP level may reflect AMPK activation.

HER2-positive breast cancer cells were shown to display AMPK activation and in 2015 AMPK was found to regulate HER2 activity [26, 27]. Therefore we focus on measuring the adenosine monophosphate (AMP) level in the tumor areas of gastroesophageal adenocarcinomas. So far no in situ method is suitable for the detection of AMP, this is a domain of mass spectrometry, more specifically mass spectrometry imaging. Previous studies showed the feasibility for measuring AMP by MALDI imaging in different kind of tissues [28–31]. Buck et al. [8] verified the detection of AMP in FFPE tissues by MSMS experiments. In addition, a successful analysis was also formerly been performed liquid based for AMP in FFPE tissues [32]. Thus, we used MALDI imaging as a further modality to increase the information received from FISH analysis and hence to get an enhanced disease prognosis.

In the present study, we combined metabolic information from MALDI imaging data with genetic information from HER2 FISH analysis of the very same tissue sections and found that HER2 status testing by FISH and AMP levels detected by MALDI imaging have a synergistic effect for prognosis.

Materials and methods

Human tissue samples

At all, 74 human gastroesophageal adenocarcinoma patient samples were analyzed.

Sixty-nine tissue samples of gastroesophageal adenocarcinoma were collected between 1993 and 2010 at the Department of Surgery, Klinikum Rechts der Isar, Munich, Germany. This study was approved by the local Ethics Committees.

Tissue samples were fixed for 12–24 h in 10% neutral buffered formalin whereafter specimen were embedded in paraffin using standardized automated procedures. Prior to

embedding in molten paraffin, the samples were dehydrated in increasing ethanol series and cleared using xylene. The resulting paraffin blocks from the cohort collected in Munich were then used for the preparation of a tissue microarray (TMA).

Five biopsies of human gastroesophageal adenocarcinoma, collected at the Institute of Pathology, University of Bern, Bern, Switzerland, were chosen for the establishment and validation of the workflow due to the previously found HER2 gene amplification. The usage of archival FFPE tissue for research was approved by the local ethics commission (Kantonale Ethikkommission Bern, Switzerland, 200/14).

Multimodal tissue analysis by MALDI imaging and fluorescence in situ hybridization (FISH)

The goal of this methodic work is the combination of two modalities: metabolites by MALDI imaging and gene copy number by fluorescence in situ hybridization (FISH) using one very same formalin-fixed and paraffin-embedded (FFPE) tissue section for all imaging modalities. The workflow is depicted in Fig. 1, starting with the MALDI imaging measurement followed by H&E staining. For performing the second modality, FISH, the coverglass was removed and a special washing procedure was carried out to ensure the complete elimination of mounting medium from the tissue. As a last step, data gained from MALDI imaging

and FISH were fused in order to enhance prognosis prediction in the patient cohort (Fig. 1).

Tissue preparation

Tissue sections of 4 μm thickness were cut using CM1950 cryostat (Leica Microsystems, Wetzlar, Germany) and mounted onto indium-tin-oxide (ITO) coated glass slides (Bruker Daltonik GmbH, Bremen, Germany), which were previously covered with 1:1 poly-L-lysine (Sigma-Aldrich; Taufkirchen, Germany) and 0.1% Nonidet P-40 (Sigma-Aldrich; Taufkirchen, Germany). For deparaffinization, sections were incubated at 70 °C for 1 h and washed twice in xylene for 8 min. Prior MALDI matrix application, tissue sections were air-dried on a heating plate at 35 °C for 1 min and scanned using a flatbed scanner in order to acquire digital tissue images for co-registration purposes. Subsequently, the samples were covered with 10 mg/mL 9-aminoacridine matrix (Sigma-Aldrich) in 70% methanol (purity $\geq 99.9\%$), using a SunCollect sprayer (Sunchrom, Friedrichsdorf, Germany) according to Ly et al. [33]. In detail, the following preferences were applied for the automatic sprayer: vial distance of 0.50 mm for the X direction and 2.00 mm for the Y direction, 20 mm Z-position and offset of the spray head, and medium X/Y speed. The matrix was deposited in eight layers using variable increasing spray rates. Following spray rates were used: Layer 1: 10 $\mu\text{l}/\text{min}$, layer 2: 20 $\mu\text{l}/\text{min}$, layer 3: 30 $\mu\text{l}/\text{min}$, layer 4–8: 40 $\mu\text{l}/\text{min}$. At all, the whole procedure is resulting in a total amount of 0.16 mg/cm² 9-aminoacridine.

MALDI imaging

MALDI imaging was performed using a Solarix 7 T FT-ICR mass spectrometer (Bruker Daltonik GmbH, Bremen, Germany) at a spatial resolution of 60 μm in negative ion mode in the mass range of m/z 50–1000, whereby 50 laser shots were accumulated for each position measured. The software packages FlexImaging 4.0 and SolarixControl 3.0 (Bruker Daltonik GmbH, Bremen, Germany) were applied for data generation and visualization as previously described [33, 34].

After MALDI measurement, matrix was removed by a washing step in 70% ethanol for 1 min and subsequently stained with histological hematoxylin and eosin staining as described previously. Coverglass was mounted using Pertex mounting medium (Medite GmbH, Burgdorf, Germany).

For digitalization slides were scanned at 20x objective magnification with a slide scanner (Mirax Desk, Carl Zeiss MicroImaging GmbH, Jena, Germany). For co-registration with MALDI imaging data, the images were imported into the FlexImaging 4.0 software (Bruker Daltonik GmbH, Bremen, Germany).

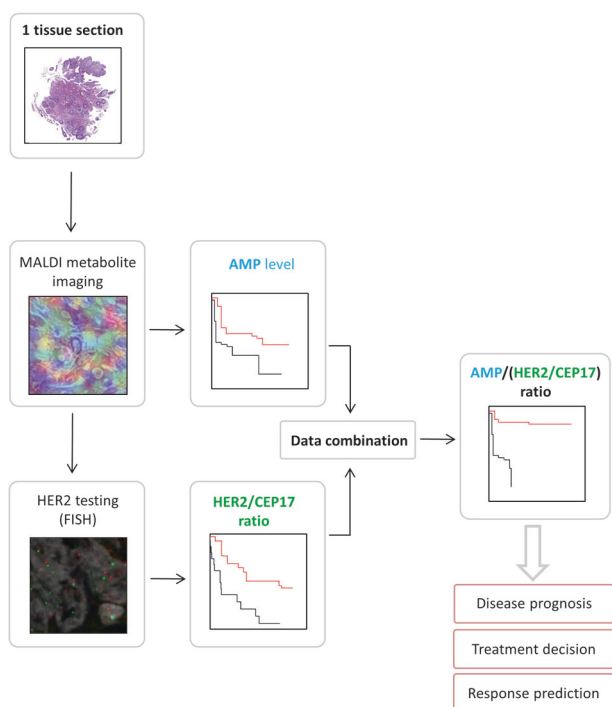


Fig. 1 The workflow of MALDI imaging with H&E staining, followed by a FISH analysis on the very same tissue section

FISH experiment

The FISH experiment was performed using the tissue sections, which were stained with hematoxylin and eosin after the MALDI imaging measurement (Fig. 1).

Slides were incubated in xylene at room temperature for 12 h before coverglass was removed. Subsequently further washing steps in xylene and isopropyl alcohol, each for the duration of 1 h, were carried out. This washing procedure was followed by a series of decreasing ethanol concentrations from 100% down to 50%, whereas the sections were immersed for 5 min at each step before they were transferred into demineralized water.

After incubating for 5 min in PBS (Sigma-Aldrich; Taufkirchen, Germany) at room temperature, the sections were boiled in citrate buffer containing 0.1 M citric acid (Sigma-Aldrich; Taufkirchen, Germany) and 0.1 M sodium citrate (Sigma-Aldrich; Taufkirchen, Germany) for 20 min using a microwave oven at 350 W. Afterwards the sections were washed in PBS and incubated in Pronase E 0.05 % (Sigma-Aldrich; Taufkirchen, Germany) for 5 min at 37 °C. Again one washing step in PBS was performed before the sections were dehydrated in ascending alcohol series, 5 min in each concentration, at -20 °C. The sections were then air-dried at room temperature and heated on a heat plate at 37 °C for 1 min.

HER2-CEP17 probes (PathVysion HER2 DNA Probe Kit II, Abbott, Illinois, USA) were added to the slide, still placed on a 37 °C heat plate, covered with Fixogum rubber cement (Marabu) and stored in the dark. Denaturation happened simultaneously by increasing the temperature of the heat plate to 75 °C for 8 min. For hybridization, slides were kept in a humid atmosphere at 37 °C for 16 h. After the incubation, slides were washed by short immersion in 2x SSC (Sigma-Aldrich; Taufkirchen, Germany) containing 0.3% Nonidet P-40 at room temperature and for 2 min in 2x SSC containing 0.3% Nonidet P-40 at 73 °C. After air-drying, slides were stained using Hoechst (Sigma-Aldrich; Taufkirchen, Germany) at room temperature and air-dried again. Coverglasses were mounted using Vectashield mounting medium (Biozol, Eching, Germany).

The kit consists of directly labeled, fluorescent DNA probes specific for the HER2 gene locus (17q11.2-q12) and a DNA probe specific for the α -satellite DNA sequence at the centromeric region of chromosome 17 (17p11.1-q11.1).

FISH analysis of the biopsy sections without previous MALDI imaging was performed in equal manner at Bern University in Switzerland.

Evaluation of the FISH experiment included counting of the fluorescent labels for gene copy numbers and centromeric region. Therefore a Z1 ZEISS Axioimager microscope (Zeiss, Jena, Germany) with a x63 magnification water objective was used.

Data analysis

For processing of the MALDI imaging data a MATLAB script using the bioinformatics and image processing toolboxes (v.7.10.0, MathWorks, Natick, MA, USA) was employed. Spectra which were exported by the FlexImaging 4.0 software (Bruker Daltonik GmbH, Bremen, Germany) underwent baseline subtraction, resampling, and smoothing as described previously [8, 34]. A signal-to-noise threshold of 2 was used and isotope peaks were excluded automatically. Human Metabolome Database (HMDB, Version 4.0, 114,098 metabolites included) was employed for the identification of *m/z* species with a mass tolerance of 3 ppm. The resulting peak intensity of AMP was exported to Microsoft Excel for data fusion with the FISH results.

The HER2 FISH approach was evaluated according to the recent guidelines [11]. The signals for HER2 gene loci and CEP17 centromere of 20 non-overlapping tumor cell nuclei were counted manually. The ratio HER2/CEP17 was calculated using Excel, whereas a HER2/CEP17 ratio ≥ 2.0 was considered as HER2 amplification [11]. Samples displaying a HER2/CEP17 ratio < 2.0 were classified as non-amplified. Furthermore, we differentiated the non-amplified samples into two groups. A HER2/CEP17 ratio ≥ 1.1 and < 2 was classified as low-level copy number gain, whereas a HER2/CEP17 ratio < 1.1 shows the status of a normal diploid nucleus [13, 35].

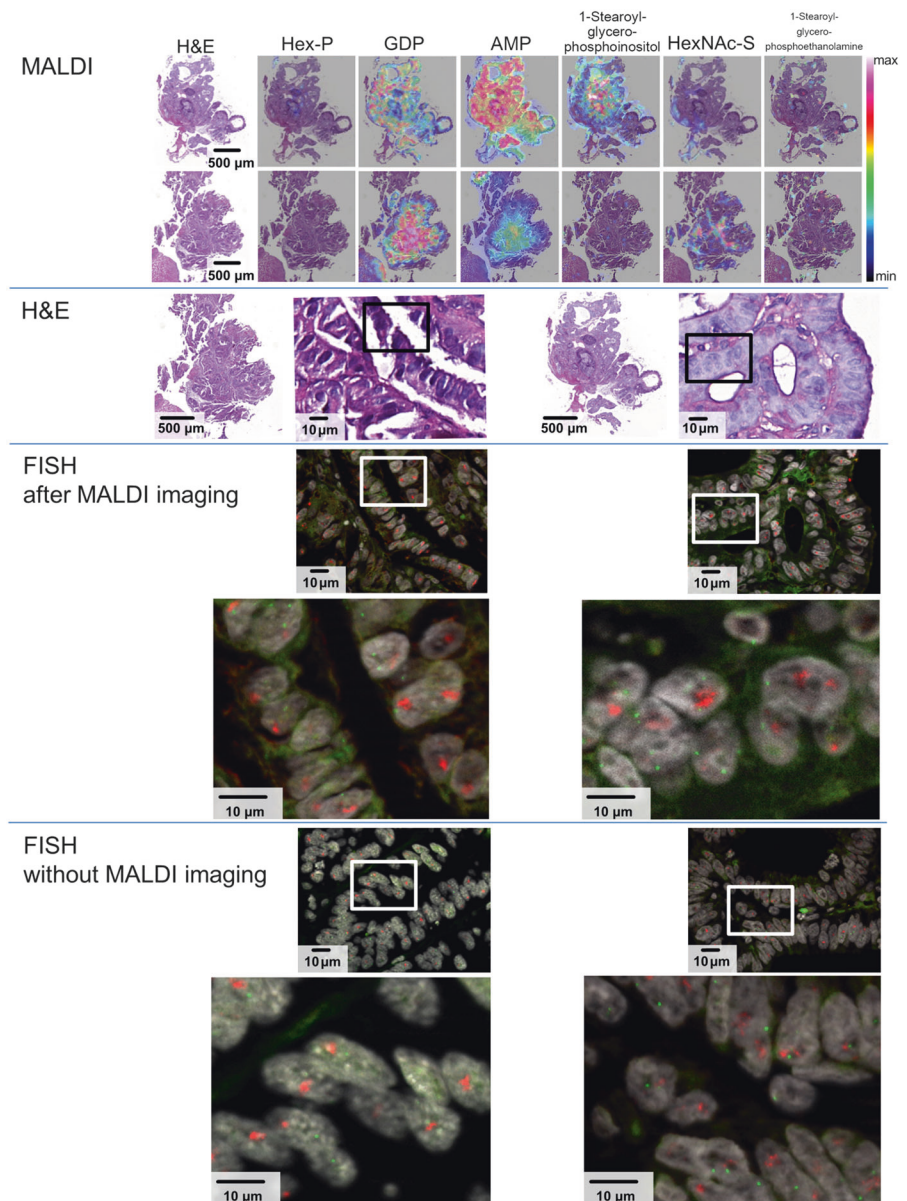
Kaplan–Meier survival tests were performed using R statistics software and Prism was used for correlation plotting.

Results

Nuclear morphology of formalin-fixed and paraffin-embedded (FFPE) tissue is unaffected after MALDI imaging

Human gastroesophageal adenocarcinoma biopsies, in the form of formalin-fixed and paraffin-embedded (FFPE) tissues, were used for validation of the fluorescence in situ hybridization (FISH) analysis either following MALDI imaging measurement or without a previous MALDI imaging measurement. One section of each biopsy sample was processed for MALDI FT-ICR metabolite imaging. Molecule visualizations resulting from the MALDI imaging approach are displayed in Fig. 2. The molecule signals follow the tissue morphology and, after co-registration with the H&E staining, it is possible to precisely allocate mass signals with tissue structures (Fig. 2). The overlay of MALDI imaging and H&E enables the identification and evaluation of specific tissue structures, e.g., tumor cell regions.

Fig. 2 Biopsies of gastroesophageal adenocarcinoma patients were measured using MALDI FT-ICR imaging for the analysis of metabolites followed by H&E staining. The MALDI visualization of Hex-P (hexose phosphate), GDP (guanosine diphosphate), AMP (adenosine monophosphate), and further molecules are depicted using heatmap coloring in the first block. The MALDI imaging heatmap pictures are displayed as merged figures with the H&E stainings as background to enable morphologic correlation. FISH analysis of both biopsies was performed subsequent to the MALDI imaging procedure. Both biopsies showed HER2 amplification when detected after the MALDI imaging workflow or when performed exclusively. For validation, consecutive sections of the very same biopsies were analyzed by FISH exclusively



After analysis of the combined MALDI imaging, the coverglass was removed and FISH analysis was performed in order to detect HER2 gene amplification (Fig. 1). Figure 2 shows the direct allocation of tissue structures, precisely identifiable in the H&E staining, with the fluorescence microscopy image of the FISH analysis. In FISH analysis, nuclei are the only cell components, which are stained (gray) (Fig. 2). The HER2 gene loci and the centromere region of chromosome 17 are fluorescent labeled by hybridization with red fluorescent probe (HER2) and green fluorescent probe (CEP17), which enables counting of signal numbers and thusly calculating the HER2/CEP17 signal ratio. There are two major preconditions for reliable HER2 testing. Nuclei must be stained clearly in order to allocate all signals belonging to each

nucleus and fluorescence signals for both, HER2 probe and centromere probe CEP17, have to be clearly visible to enable distinct recognition of single signals.

The FISH analysis was evaluable even after the MALDI imaging procedure. Single fluorescence signals, even in non-amplified tissues were clearly visible and enumeration was possible just as in tissues, which were not used for the MALDI imaging procedure. The nuclear morphology was clear and completely unaffected by MALDI imaging. The Hoechst nuclear staining allowed the detection of tumor areas and even cytomorphological details of the nuclear structure remained unchanged after MALDI imaging.

The ratios of HER2 gene locus (red) and centromeric region of chromosome 17 (green) signals were calculated, whereas a ratio ≥ 2.0 was designated as HER2 amplification

[11]. In the FISH experiment we found high-level amplification of HER2 gene copy number in both biopsies (Fig. 2). The FISH experiment that was performed after MALDI imaging and H&E staining resulted in excellent signals, which allowed a very precise detection of gene amplifications (Fig. 2).

HER2 testing by FISH after MALDI imaging and without MALDI imaging reveals equal results

In order to validate the findings from the samples, which underwent the MALDI imaging pipeline, consecutive reference sections of five biopsies were analyzed by FISH as a reference, not undergoing the procedure of MALDI imaging and H&E staining. The FISH experiment was evaluated identically for the sections, which underwent the MALDI imaging protocol as for those reference sections

without previous MALDI imaging procedure. All biopsies after MALDI imaging showed HER2 amplification. The quantitative evaluation of the approaches is displayed in Fig. 3. Signal counts of HER2 and CEP17 of five biopsies were compared after the MALDI workflow and without previous MALDI and the HER2/CEP17 signal ratio was calculated. For biopsy 1, an average of 8.0 HER2 signals was detected after MALDI and 10.0 signals without MALDI workflow. CEP17 signal count revealed 1.6 and 1.5 signals per nucleus, respectively. The resulting HER2/CEP17 signal ratios were 5.0 and 6.7. Biopsy 2 showed HER2 amplification with a mean HER2 signal count of 16.8 after MALDI and 15.4 without MALDI. With a CEP17 number of 2.0 and 1.8, the resulting HER2/CEP17 signal ratios were 8.4 and 8.6. The results for biopsy 3, 4, and 5 were also equal after MALDI imaging and were shown in Table 1. Additional exemplary pictures of FISH analysis for

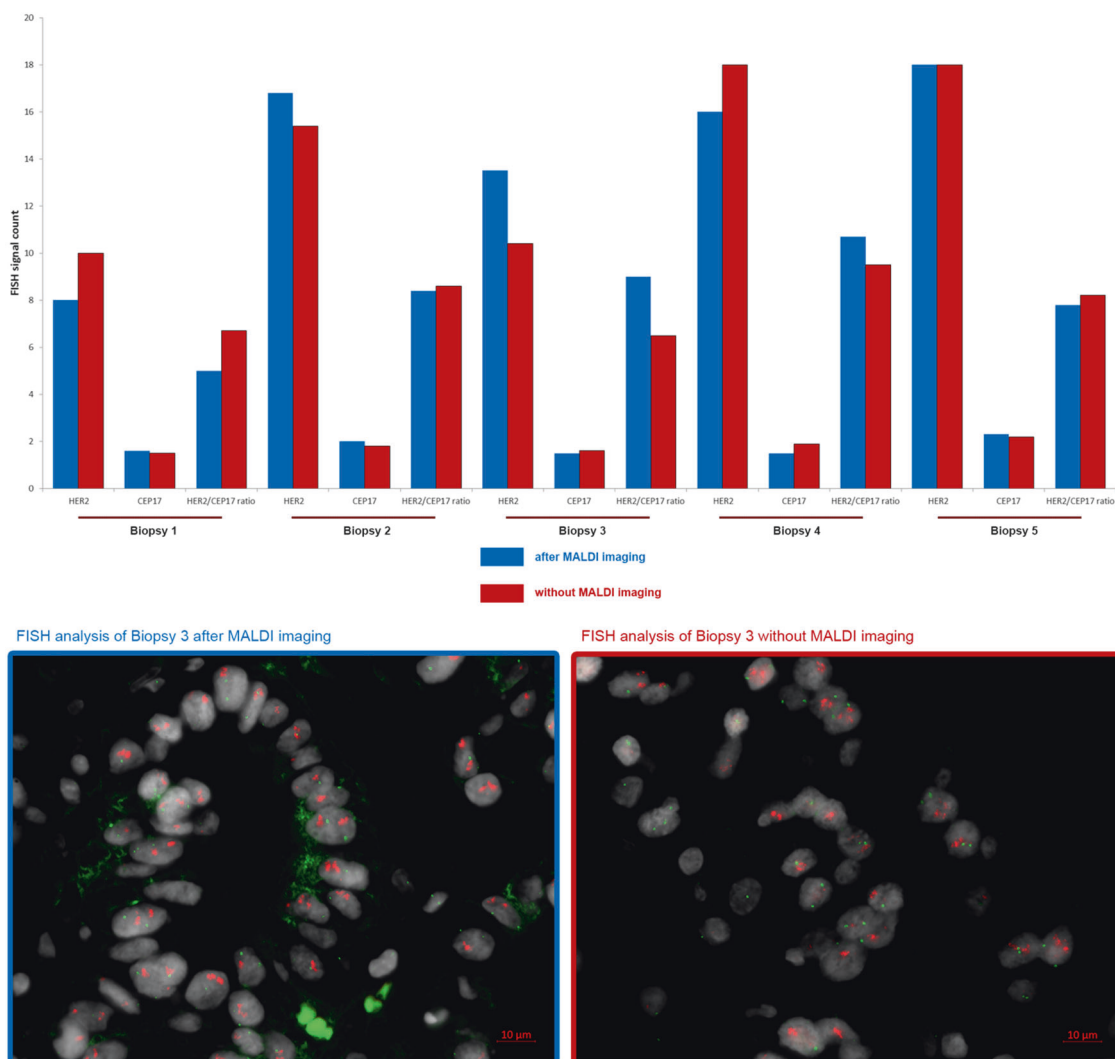


Fig. 3 HER2 signals, CEP17 signals, and HER2/CEP17 ratios derived from FISH analysis of five human gastroesophageal cancer biopsies. FISH signals from 20 tumor cell nuclei were enumerated manually in

biopsies, which were analyzed by FISH after the MALDI imaging procedure or without previous MALDI imaging, respectively. The shown examples for FISH are referring to Biopsy 3

Table 1 Comparison of FISH results after and without MALDI imaging

Characteristic	After MALDI imaging	Without MALDI imaging
Biopsy 1		
HER2 [mean signals]	8.0	10.0
CEP17 [mean signals]	1.6	1.5
HER2/CEP17 ratio	5.0	6.7
Biopsy 2		
HER2 [mean signals]	16.8	15.4
CEP17 [mean signals]	2.0	1.8
HER2/CEP17 ratio	8.4	8.6
Biopsy 3		
HER2 [mean signals]	13.5	10.4
CEP17 [mean signals]	1.5	1.6
HER2/CEP17 ratio	9.0	6.5
Biopsy 4		
HER2 [mean signals]	16.0	18.0
CEP17 [mean signals]	1.5	1.9
HER2/CEP17 ratio	10.7	9.5
Biopsy 5		
HER2 [mean signals]	18.0	18.0
CEP17 [mean signals]	2.3	2.2
HER2/CEP17 ratio	7.8	8.2

all biopsies can be seen in Supplementary Fig. 1. Comparing the quality of the tissue after the combined workflow with the tissue that underwent only the FISH experiment, there is no difference in quality and evaluability.

HER2 testing after MALDI imaging allows accurate disease prognosis prediction

A tissue microarray containing 69 human gastroesophageal adenocarcinoma patient samples was analyzed using the established pipeline of MALDI imaging followed by FISH. Figure 4 displays the distribution of several molecules measured by MALDI imaging. As established for the biopsies, the TMA underwent FISH after the MALDI imaging procedure following the same workflow as described above. The results from the FISH analysis are presented in Fig. 5. Tissue cores in Fig. 5a, b showed low/medium level HER2 amplifications, while the core in Fig. 5c was a highly amplified sample. The samples in Fig. 5d, e, f were found to be not HER2 amplified.

In all, nine tissue cores were found to be HER2 amplified, while 60 were not amplified. In the group of non-amplified cores, 18 were found to show low-level copy number gain while 42 were diploid without copy number

gain. Average HER2 signal counts varied from 0.8 to 15.4, the average HER2 signal count of all observed cases was 2.4 signals per nucleus.

The FISH evaluation of the tissue microarray was analyzed statistically using the Kaplan–Meier survival test (Fig. 6). Hereby a significant ($p = 0.0350$) difference in patient survival was found, outlining HER2/CEP17 signal ratio as a marker for patient survival (Fig. 6a).

Adenosine monophosphate is a prognostic factor in gastroesophageal adenocarcinoma

In the MALDI imaging approach, the H&E staining was used for the determination of tumor regions. Thus, it was possible to extract mass spectra specifically from the tumor areas for analysis. We focused on the peak intensity of adenosine monophosphate (AMP, m/z 346.0570), which we expected to serve as prognostic marker. AMP signal intensity allowed significant prediction of patient survival ($p = 0.00206$). Hereby the mass intensity was found to be higher in the good prognosis group, while signal intensity was weak in the poor prognosis group (Fig. 6b). In general, average AMP peak intensities varied between 0 and 7.59. In 39 cases mean AMP intensity was found to be below 1.0 and 2 cases showed an intensity of >5 . The intensity of 28 cases was in the medium range between 1.0 and 5.0. The overall average AMP intensity is 1.42. In the samples, which were stratified as poor survivors (Fig. 6b), AMP signal intensity was below 0.15.

Data combination of FISH and MALDI has a synergistic effect on prognosis

According to our hypothesis, we combined the data revealed from both approaches, AMP signal intensity by MALDI imaging and gene amplification by FISH, using the ratio of the mass intensity and the HER2/CEP17 signal ratio, lead to an improvement in the significance of survival analysis with $p = 0.000002875$. The patients in the good prognosis group show a higher AMP/FISH ratio than the patients in the poor prognosis group. The calculated threshold to stratify patient survival was 0.22 (Fig. 6c).

In Supplementary Fig. 2, AMP signal intensities from MALDI imaging were plotted against the HER2 signal count revealed from FISH in order to detect whether there is a correlation of the abundance of both features. Each datapoint represents a single patient. The random distribution of the datapoints in the plot depicts the fact that both parameters do not correlate with each other ($p = 0.5020$). In addition, the HER2/CEP17 ratio was also tested for correlation and reached not a significant level (Supplementary Fig. 3, $p = 0.2183$).

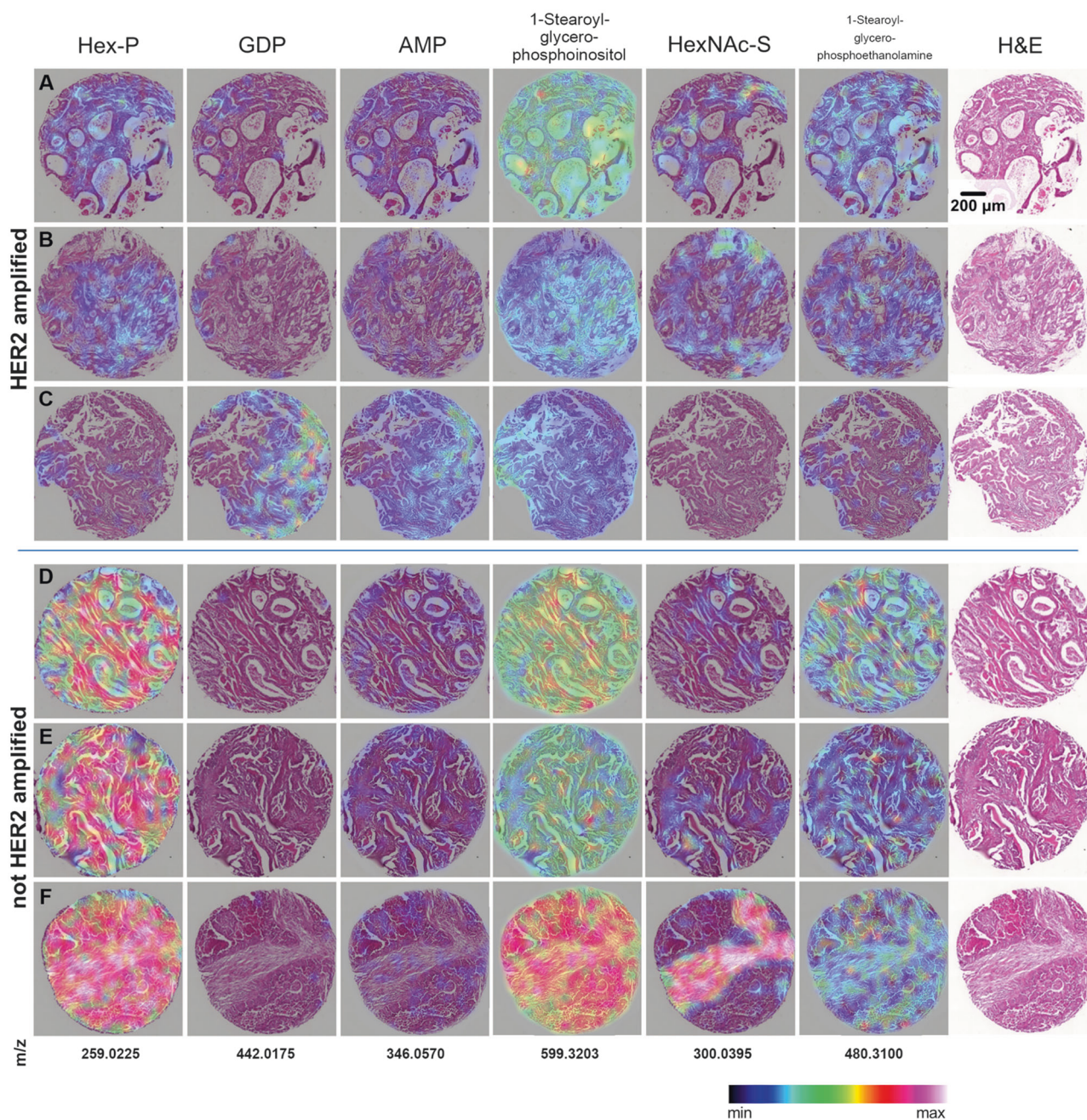


Fig. 4 A tissue microarray (TMA) containing 69 human gastroesophageal adenocarcinoma samples was measured by MALDI FT-ICR metabolome imaging. Molecules, e.g., Hex-P (hexose phosphate), GDP (guanosine diphosphate), AMP (adenosine monophosphate), are visualized exemplarily on six tissue cores in heatmap coloring

according to the biopsies, which are displayed in Fig. 2. The samples are either HER2 amplified (upper panel) or non-amplified (lower panel). Measured m/z values of the metabolites can be obtained from the last row. The panels **a–f** refer to the same tissue cores as shown in Fig. 5

Discussion

In this study, we developed a novel combined approach which, for the first time, allows the direct correlation of findings from MALDI imaging experiments and essential histological staining with the outcome of FISH analysis on the very same tissue section.

As example for the additional value of the method combination, we focused on measuring the AMP levels using MALDI metabolite imaging as a surrogate marker for the activity of AMP-activated kinase (AMPK), which is known to be stimulated by high AMP levels, which appear due to a lack of ATP in tumor metabolism [22]. AMPK is described to impact HER2 and has major influence on

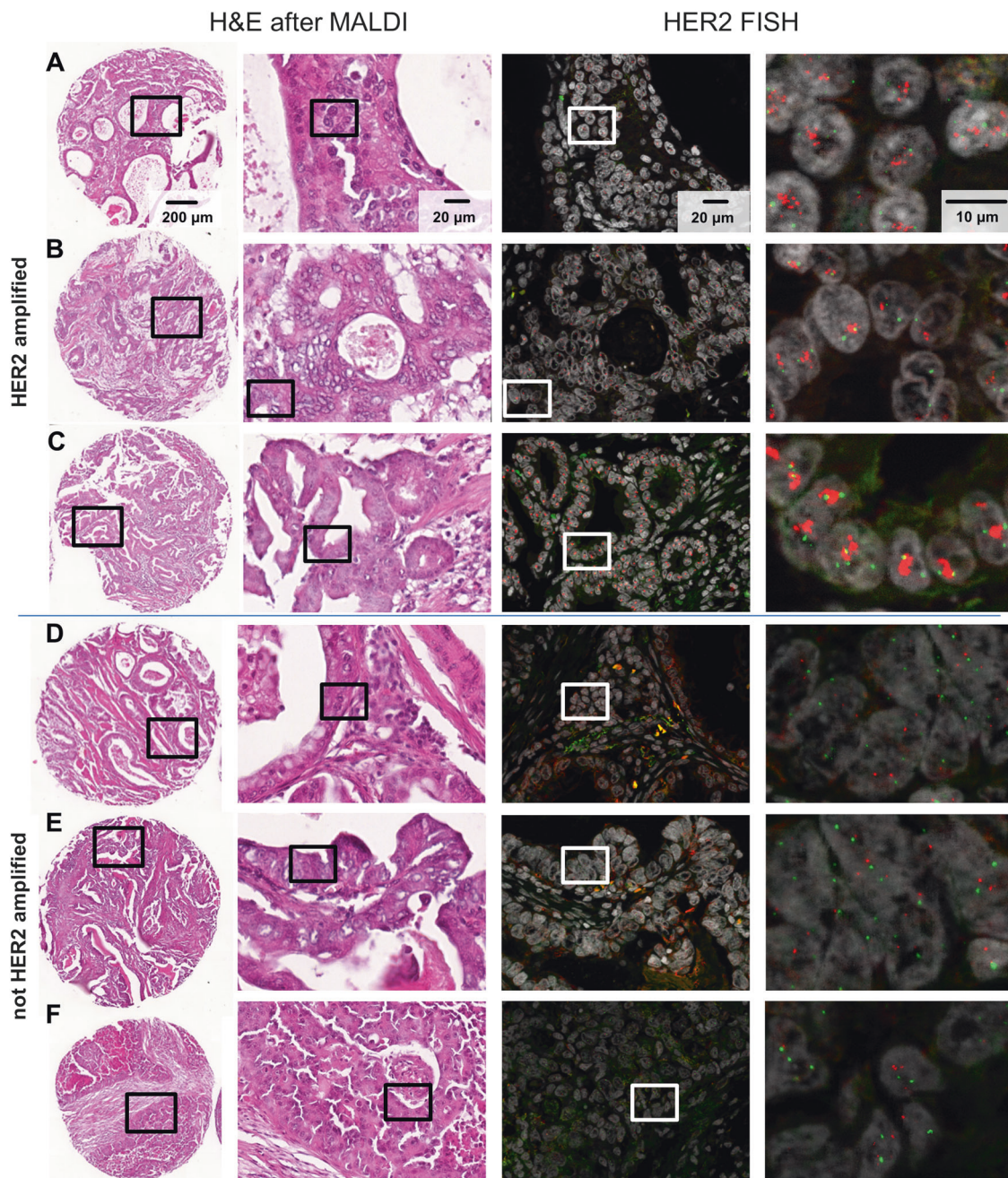


Fig. 5 After H&E staining, FISH analysis was performed on the very same TMA section. The HER2 gene locus carries a red fluorescence label, while the centromeric region of chromosome 17 is marked with a green fluorescence label. The nuclei are stained using Hoechst (gray).

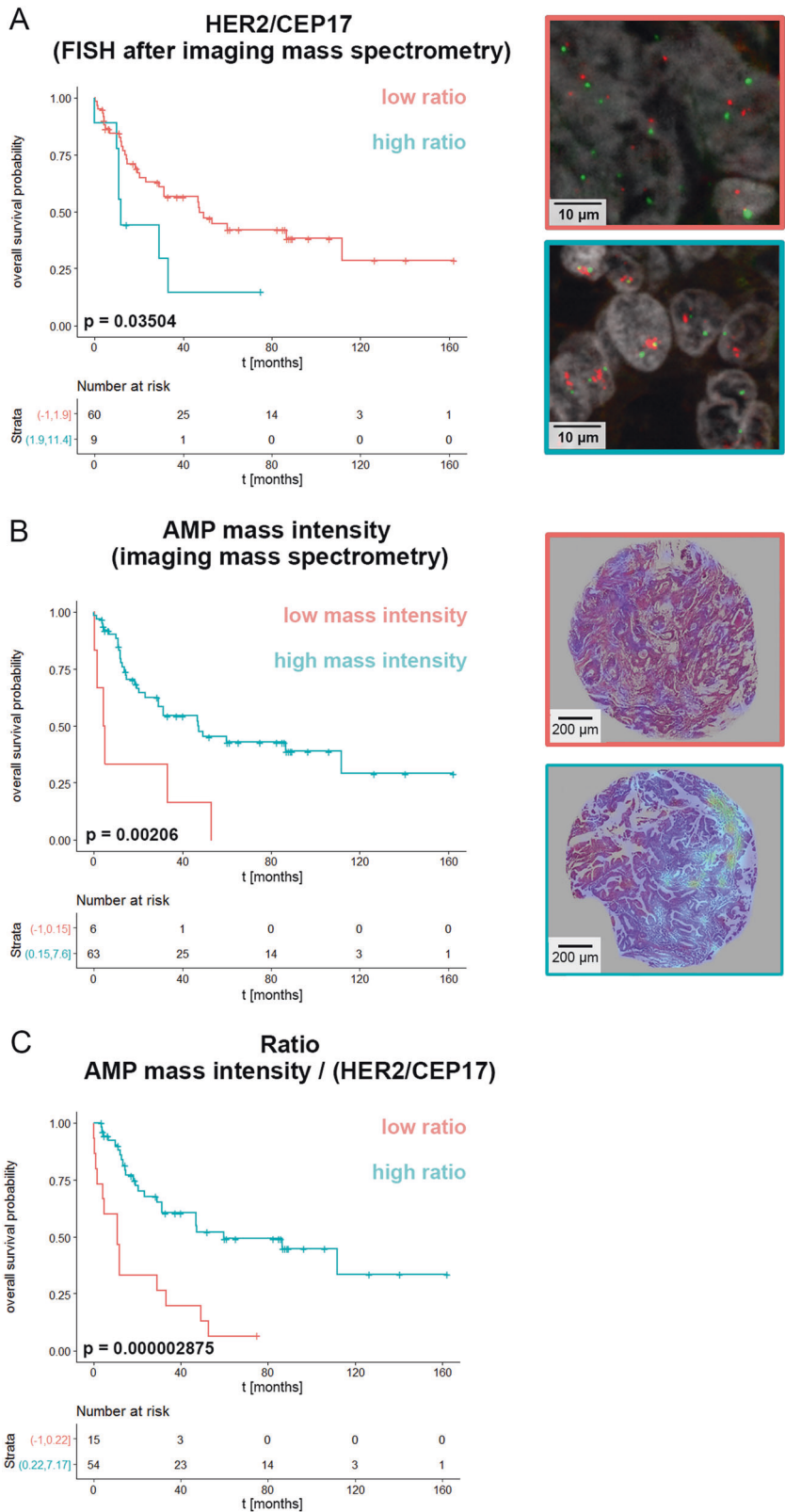
The cores shown in **a**, **b** show medium level HER2 gene amplification, whereas the core in **c** is a high-amplified tissue sample. The cores displayed in **d**, **e**, **f** are not amplified

tumor growth and progression [23, 27]. Jhaveri et al. [27] described a decreased activation of HER2 and EGFR caused by AMPK in human breast cancer cell lines and xenograft tumors. The mechanistical study in breast cancer cell lines showed that AMPK directly inhibits the activity of HER2 via phosphorylation. As AMPK is activated by an increased cellular AMP level [36], it could be, that an increased level of AMP can serve as a surrogate marker for

AMPK activity and thus it might also work as a predictor for tumor cell progression by indirectly reflecting the activity of HER2. Of note, our results are not able to provide a causal explanation of an impact of AMP to HER2 signaling.

As HER2 gene amplification and AMP mass intensity both have the ability to differ significantly between good and poor prognosis group in the Kaplan–Meier analysis

Fig. 6 **a** Kaplan–Meier survival analysis was performed using the parameters HER2/CEP17 signal ratio from FISH analysis. The image on the top right corner shows a HER2/CEP17 FISH sample with a non-amplified diploid state (image with red border) representative for good prognosis and on the lower right corner a sample with a HER2 gene amplification (image with blue border) for poor prognosis. **b** AMP mass signal intensity from the MALDI imaging approach is able to separate patient samples as a prognostic factor. Ion distribution maps showing localization of AMP in tissue cores representative for low-mass intensity (image with red border) and high-mass intensity (image with blue border). **c** The ratio of the mass intensity of AMP and the HER2/CEP17 signal ratio lead to significant improvement of survival analysis



while not correlating to each other, the information of both parameters was combined as a ratio. Using this ratio it is possible to increase the significance level of the survival

analysis to $p = 0.000002875$. Hereby it becomes obvious, that the information from the gene amplification analysis and the mass spectrometry imaging approach together sum

up to a very precise prognosis, which is strikingly better than each method alone. The correlation plot depicted in Supplementary Fig. 2 shows that HER2 signal count and AMP level do not correlate with each other. Another possibility might be the analysis of further molecules, which are involved in this or even other pathways of tumor progression. As MALDI imaging is widely used for the detection of proteins, it is another opportunity to combine protein measurements with FISH analysis in future studies.

This approach was established and validated using human gastroesophageal adenocarcinoma biopsies. A comparison of a FISH analysis after MALDI imaging with a reference FISH analysis without previous MALDI imaging using consecutive sections of the same biopsies was performed (Fig. 3 and Table 1). Hereby the results from both approaches revealed were similar. Most notably, after the performance of the whole protocol, cell structure is still preserved and FISH results remain as correct and reliable as when performed exclusively. This result highlights the robustness of well-prepared FFPE tissues, which proved to be an outstanding source of information.

Hence, we claim that our MALDI imaging protocol leaves the tissue intact and does not influence the outcome of subsequent FISH experiments.

We demonstrate that our protocol does not only keep the tissue structure intact, but, most remarkably, it even leaves the DNA structure unimpaired and thus the FISH approach remains unaffected by the foregoing procedure.

Our results are concordant with the work of Kazdal et al. [37], which shows the combination of MALDI imaging with digital PCR, although describing the robustness of the DNA structure even after undergoing the MALDI ionization procedure. Regarding the fact, that the molecules are ionized from the tissue by an UV laser beam, it is a notable finding that the DNA is still intact to allow reliable FISH results. A combination of IR spectroscopic imaging and MALDI imaging was recently described by Neumann et al. [38], enabling more advanced tissue analysis. Here, MALDI imaging measurement were carried out before the very same tissue was analyzed by IR spectroscopic imaging, as the gently ionization method did not destroy the tissue [38]. Owing to these findings and because we expect a loss of metabolites during the washing steps of the FISH protocol, we aimed to develop a protocol, which enables the performance of FISH analysis after the MALDI imaging procedure.

The described combined tissue analysis approach is established for tissue biopsies. As biopsies represent the standard material used in clinical diagnostics and our approach does not require further sections of the anyways limited material, our combined method is very suitable for the use in the clinical setting [39]. MALDI imaging was

described as a promising tool for clinical diagnostics, as well as for clinical research [40, 41].

Our workflow consists of a new multimodal procedure of tissue analytics, which allows molecular feature extraction by mass spectrometry imaging, and phenotypic and cytogenetic feature extraction by digital image analysis, resulting in highly improved prognosis estimation. Thus, the overall information that can be gained from one tissue section is extended, and, in combination with clinical data, including survival and response, this combined workflow represents a promising tool for further biomarker research. Additionally, the present work shows the prognostic value of MALDI imaging. As disease prognosis is significantly improved by the addition of MALDI imaging data, the described multimodal method might have potential to improve response prediction as well.

Acknowledgements We thank Ulrike Buchholz, Claudia-Mareike Pflüger, Andreas Voss, Gabriele Mettenleiter, Cristina Huebner Freitas, and Elenore Samson for excellent technical assistance.

Funding The study was funded by the Ministry of Education and Research of the Federal Republic of Germany (BMBF; Grant Nos. 01ZX1610B and 01KT1615), the Deutsche Forschungsgemeinschaft (Grant Nos. SFB 824 TP C04, CRC/TRR 205 S01) and the Deutsche Krebshilfe (No. 70112617) to A. Walch.

Compliance with ethical standards

Conflict of interest The authors declare that they have no conflict of interest.

Publisher's note: Springer Nature remains neutral with regard to jurisdictional claims in published maps and institutional affiliations.

References

1. Wu M, Shu J. Multimodal molecular imaging: current status and future directions. *Contrast Media Mol Imaging*. 2018;2018:1382183.
2. Kircher MF, Mahmood U, King RS, Weissleder R, Josephson L. A multimodal nanoparticle for preoperative magnetic resonance imaging and intraoperative optical brain tumor delineation. *Cancer Res*. 2003;63:8122–5.
3. Takakusagi Y, Naz S, Takakusagi K, Ishima M, Murata H, Ohta K, et al. A multimodal molecular imaging study evaluates pharmacological alteration of the tumor microenvironment to improve radiation response. *Cancer Res*. 2018;78:6828–37.
4. Buchberger AR, DeLaney K, Johnson J, Li L. Mass spectrometry imaging: a review of emerging advancements and future insights. *Anal Chem*. 2018;90:240–65.
5. Schulz S, Becker M, Groseclose MR, Schadt S, Hopf C. Advanced MALDI mass spectrometry imaging in pharmaceutical research and drug development. *Curr Opin Biotechnol*. 2019;55: 51–9.
6. Buck A, Aichler M, Huber K, Walch A. In situ metabolomics in cancer by mass spectrometry imaging. *Adv Cancer Res*. 2017;134:117–32.
7. Kriegsmann K, Longuespee R, Hundemer M, Zgorzelski C, Casadonte R, Schwamborn K, et al. Combined immunohistochemistry

- after mass spectrometry imaging for superior spatial information. *Proteomics Clin Appl*. 2019;13:e1800035.
8. Buck A, Ly A, Balluff B, Sun N, Gorzolka K, Feuchtinger A, et al. High-resolution MALDI-FT-ICR MS imaging for the analysis of metabolites from formalin-fixed, paraffin-embedded clinical tissue samples. *J Pathol*. 2015;237:123–32.
 9. Boekhout AH, Beijnen JH, Schellens JH. Trastuzumab. *Oncologist*. 2011;16:800–10.
 10. Lote H, Valeri N, Chau I. HER2 inhibition in gastro-oesophageal cancer: A review drawing on lessons learned from breast cancer. *World J Gastrointest Oncol*. 2018;10:159–71.
 11. Bartley AN, Washington MK, Colasacco C, Ventura CB, Ismaila N, Benson AB, et al. HER2 testing and clinical decision making in gastroesophageal adenocarcinoma: guideline from the College of American Pathologists, American Society for Clinical Pathology, and the American Society of Clinical Oncology. *J Clin Oncol*. 2017;35:446–64.
 12. Lordick F, Al-Batran SE, Dietel M, Gaiser T, Hofheinz RD, Kirchner T, et al. HER2 testing in gastric cancer: results of a German expert meeting. *J Cancer Res Clin Oncol*. 2017;143:835–41.
 13. Rauser S, Weis R, Braselmann H, Feith M, Stein HJ, Langer R, et al. Significance of HER2 low-level copy gain in Barrett's cancer: implications for fluorescence in situ hybridization testing in tissues. *Clin Cancer Res*. 2007;13:5115–23.
 14. Hagemann IS. Molecular testing in breast cancer: a guide to current practices. *Arch Pathol Lab Med*. 2016;140:815–24.
 15. Sauter G, Lee J, Bartlett JM, Slamon DJ, Press MF. Guidelines for human epidermal growth factor receptor 2 testing: biologic and methodologic considerations. *J Clin Oncol*. 2009;27:1323–33.
 16. Burandt E, Sauter G. HER2-ASCO-guidelines. *Der Pathologe*. 2010;31:285–91.
 17. Fu X, Zhang Y, Yang J, Qi Y, Ming Y, Sun M, et al. Efficacy and safety of trastuzumab as maintenance or palliative therapy in advanced HER2-positive gastric cancer. *Onco Targets Ther*. 2018;11:6091–100.
 18. Suter TM, Procter M, van Veldhuisen DJ, Muscholl M, Bergh J, Carlomagno C, et al. Trastuzumab-associated cardiac adverse effects in the herceptin adjuvant trial. *J Clin Oncol*. 2007;25:3859–65.
 19. de Azambuja E, Procter MJ, van Veldhuisen DJ, Agbor-Tarh D, Metzger-Filho O, Steinseifer J, et al. Trastuzumab-associated cardiac events at 8 years of median follow-up in the Herceptin Adjuvant trial (BIG 1-01). *J Clin Oncol*. 2014;32:2159–65.
 20. Gomez-Martin C, Lopez-Rios F, Aparicio J, Barriuso J, Garcia-Carbonero R, Pazo R, et al. A critical review of HER2-positive gastric cancer evaluation and treatment: from trastuzumab, and beyond. *Cancer Lett*. 2014;351:30–40.
 21. Van Cutsem E, Bang YJ, Feng-Yi F, Xu JM, Lee KW, Jiao SC, et al. HER2 screening data from ToGA: targeting HER2 in gastric and gastroesophageal junction cancer. *Gastric Cancer*. 2015;18:476–84.
 22. DeBerardinis RJ, Chandel NS. Fundamentals of cancer metabolism. *Sci Adv*. 2016;2:e1600200.
 23. Shackelford DB, Shaw RJ. The LKB1-AMPK pathway: metabolism and growth control in tumour suppression. *Nat Rev Cancer*. 2009;9:563–75.
 24. Mihaylova MM, Shaw RJ. The AMPK signalling pathway coordinates cell growth, autophagy and metabolism. *Nat Cell Biol*. 2011;13:1016–23.
 25. Lin SC, Hardie DG. AMPK: sensing glucose as well as cellular energy status. *Cell Metab*. 2018;27:299–313.
 26. Baumann J, Kokabee M, Wong J, Balasubramaniyam R, Sun Y, Conklin DS. Global metabolite profiling analysis of lipotoxicity in HER2/neu-positive breast cancer cells. *Oncotarget*. 2018;9:27133–50.
 27. Jhaveri TZ, Woo J, Shang X, Park BH, Gabrielson E. AMP-activated kinase (AMPK) regulates activity of HER2 and EGFR in breast cancer. *Oncotarget*. 2015;6:14754–65.
 28. Benabdellah F, Touboul D, Brunelle A, Laprevote O. In situ primary metabolites localization on a rat brain section by chemical mass spectrometry imaging. *Anal Chem*. 2009;81:5557–60.
 29. Miyamoto S, Hsu CC, Hamm G, Darshi M, Diamond-Stanic M, Declèves AE, et al. Mass spectrometry imaging reveals elevated glomerular ATP/AMP in diabetes/obesity and identifies sphingomyelin as a possible mediator. *EBioMedicine*. 2016;7:121–34.
 30. Wang X, Han J, Hardie DB, Yang J, Pan J, Borchers CH. Metabolomic profiling of prostate cancer by matrix assisted laser desorption/ionization-Fourier transform ion cyclotron resonance mass spectrometry imaging using Matrix Coating Assisted by an Electric Field (MCAEF). *Biochim Biophys Acta Proteins Proteom*. 2017;1865:755–67.
 31. Liu H, Li W, He Q, Xue J, Wang J, Xiong C, et al. Mass spectrometry imaging of kidney tissue sections of rat subjected to unilateral ureteral obstruction. *Sci Rep*. 2017;7:41954.
 32. Cacciatore S, Zadra G, Bango C, Penney KL, Tyekucheva S, Yanes O, et al. Metabolic profiling in formalin-fixed and paraffin-embedded prostate cancer tissues. *Mol Cancer Res*. 2017;15:439–47.
 33. Ly A, Buck A, Balluff B, Sun N, Gorzolka K, Feuchtinger A, et al. High-mass-resolution MALDI mass spectrometry imaging of metabolites from formalin-fixed paraffin-embedded tissue. *Nat Protoc*. 2016;11:1428–43.
 34. Kunzke T, Balluff B, Feuchtinger A, Buck A, Langer R, Luber B, et al. Native glycan fragments detected by MALDI-FT-ICR mass spectrometry imaging impact gastric cancer biology and patient outcome. *Oncotarget*. 2017;8:68012–25.
 35. Hicks DG, Tubbs RR. Assessment of the HER2 status in breast cancer by fluorescence in situ hybridization: a technical review with interpretive guidelines. *Hum Pathol*. 2005;36:250–61.
 36. Hardie DG. AMP-activated protein kinase: an energy sensor that regulates all aspects of cell function. *Genes Dev*. 2011;25:1895–908.
 37. Kazdal D, Longuespee R, Dietz S, Casadonte R, Schwamborn K, Volckmar AL, et al. Digital PCR after MALDI-mass spectrometry imaging to combine proteomic mapping and identification of activating mutations in pulmonary adenocarcinoma. *Proteomics Clin Appl*. 2019;13:e1800034.
 38. Neumann EK, Comi TJ, Spegazzini N, Mitchell JW, Rubakhin SS, Gillette MU, et al. Multimodal chemical analysis of the brain by high mass resolution mass spectrometry and infrared spectroscopic imaging. *Anal Chem*. 2018;90:11572–80.
 39. Longuespee R, Casadonte R, Schwamborn K, Reuss D, Kazdal D, Kriegsmann K, et al. Proteomics in pathology. *Proteomics*. 2018;18:1–7.
 40. Kriegsmann J, Kriegsmann M, Casadonte R. MALDI TOF imaging mass spectrometry in clinical pathology: a valuable tool for cancer diagnostics (review). *Int J Oncol*. 2015;46:893–906.
 41. Addie RD, Balluff B, Bovee JV, Morreau H, McDonnell LA. Current state and future challenges of mass spectrometry imaging for clinical research. *Anal Chem*. 2015;87:6426–33.